Production of the 1385-MeV $(Y_1^*)^0$ in 1.5-BeV/c π^- p Interactions*

L. J. CURTIS, C. T. COFFIN, D. I. MEYER, AND K. M. TERWILLIGER
The University of Michigan, Ann Arbor, Michigan
(Received 15 July 1963)

The reaction 1.508-BeV/c $\pi^-+p \rightarrow K^0+\Lambda+\pi^0$ has been studied in a spark chamber experiment; 127 events of this type were obtained. The reaction is dominated by production of the $(Y_1^*)^0$, with parameters $M_0=1381\pm4$ MeV, $\Gamma=30\pm9$ MeV. The differential cross section for production of the $(Y_1^*)^0$ is $(6.3\pm0.9)\times[1+(0.15\pm0.27)\cos\theta-(0.35\pm0.38)\cos^2\theta]$ μb/sr; the total production cross section is (70 ± 11) μb. Decay distributions of this resonance, assuming S and P waves in the production, are consistent with spin $\frac{3}{2}$, favoring it over spin $\frac{5}{2}$ with a likelihood ratio of 10/1.

INTRODUCTION

THE 1385-MeV $\Lambda\pi$ resonance or Y_1^* has been studied in considerable detail since its discovery in 1960.[1–11] It has been shown to have a resonance width T of around 50 MeV, spin $\geq\frac{3}{2}$,[4,10,11] and the same parity as the Λ (assuming spin $\frac{3}{2}$).[10] Most of the data have been obtained using K^- beams, where just the charged modes $(Y_1^*)^\pm$ are observed. Some runs have been with K_2^0 [3] and π^- beams[5–8]; here the neutral mode can be seen, but it has not been studied separately.

This paper describes a spark chamber experiment performed at the Cosmotron to investigate the 1385 MeV $(Y_1^*)^0$ through the reaction

$$\pi^-+p \rightarrow K^0+\Lambda+\pi^0. \quad (1)$$

The beam momentum was 1.508 BeV/c, the total energy in the center-of-mass 1934 MeV, giving a center-of-mass momentum of the $(Y_1^*)^0$ of approximately 200 MeV/c, fairly close to threshold. The following sections are included in this paper: Details of the beam setup, spark chamber and counter arrangements, and the experimental run; scanning and measuring methods and results; data analysis procedures; results, including a Dalitz plot and invariant mass distributions in the $K^0\Lambda\pi^0$ final state, as well as production and decay angular distributions of the $(Y_1^*)^0$.

EXPERIMENT

Beam

The 1.5-BeV/c π beam, shown schematically in Fig. 1, was designed by Piccioni. It was a two-stage beam, with an intermediate focus. It was tuned by the hot-wire method and then with the π beam. With a $\frac{3}{4}$-in.-wide momentum defining slit at the first focus, an intensity of 8×10^3 π^-/pulse was obtained in a 1- $\times$1-in. region at the second focus, when the internal proton beam was 5×10^{10}/pulse. The momentum resolution with this slit was calculated to be $\pm0.7\%$. An intensity of $\sim10^4$/pulse was the maximum that could be tolerated through the spark chambers, because the short ($\sim$30 msec) and spiked beam spill would otherwise give instantaneous fluxes larger than one or two in one μsec, the spark chamber resolution time.

Spark Chamber and Counter Setup

The main spark chamber used in the experiment[12] is 14$\times$14 in. with 12 gaps of 0.350-in. spacing. The electrodes are 0.001-in. Al foil, and the walls Lucite picture frames. The optical system for photographing the chamber is drawn in Fig. 2. Four views of the chamber were recorded on a double frame of 35 mm Tri X Pan; the two 90° view seen in Fig. 2 were used for measuring, two other smaller angle views for resolving ambiguities.

The spark chamber and counter geometry is shown in Fig. 3. The incoming pions passed through two beam-defining counters and a small spark chamber and into a $1\frac{1}{8}$-in. liquid-hydrogen target. The target was followed by an anticoincidence counter, the main spark chamber, and then a coincidence counter. The counter system

* Supported by the U. S. Atomic Energy Commission.
[1] M. Alston, L. Alvarez, P. Eberhard, M. Good, W. Graziano, H. Ticho, and S. Wojcicki, Phys. Rev. Letters **5**, 520 (1960).
[2] J. P. Berge, P. Bastain, O. Dahl, M. Ferro-Luzzi, J. Kirz, D. H. Miller, J. J. Murray, A. H. Rosenfeld, R. D. Tripp, and M. B. Watson, Phys. Rev. Letters **6**, 557 (1961).
[3] R. K. Adair, Rev. Mod. Phys. **33**, 406 (1961). H. J. Martin, L. B. Leipuner, W. Chinowsky, F. T. Shively, and R. K. Adair, Phys. Rev. Letters **6**, 283 (1961).
[4] R. P. Ely, S. Fung, G. Gidal, Y. Pan, W. M. Powell, and H. S. White, Phys. Rev. Letters **7**, 461 (1961).
[5] A. R. Erwin, R. H. March, and W. D. Walker, Nuovo Cimento **24**, 237 (1962).
[6] D. Colley, N. Gelfand, W. Nauenberg, J. Steinberger, S. Wolf, H. Brugger, P. Kramer, and R. Plano, Phys. Rev. **128**, 1930 (1962).
[7] G. Alexander, G. R. Kalbfleisch, D. H. Miller, and D. A. Smith, Phys. Rev. Letters **8**, 447 (1962).
[8] Collaboration: Saclay, Orsay, Bari, and Bologne, *Proceedings of the Aix en Provence International Conference on Elementary Particles 1961* (Centre d'Etudes Nucléaires de Saclay, Seine et Oise, 1961), Vol. 1, p. 375.
[9] M. M. Block, E. B. Brucker, R. Gessaroli, T. Kikuchi, A. Kovacs, C. M. Meltzer, R. Kramer, M. Nussbaum, A. Pevsner, P. Schlein, R. Strand, H. O. Cohn, E. M. Harth, J. Leitner, L. Lendinara, L. Monari, and G. Puppi, Nuovo Cimento **20**, 724 (1961); J. Auman, M. M. Block, R. Gessaroli, J. Kopelman, S. Ratti, L. Grimellini, T. Kikuchi, L. Lendinara, L. Monari, and E. Harth, *Proceedings of the International Conference on High-Energy Physics, CERN* (CERN, Geneva, 1962), p. 330.
[10] J. B. Shafer, J. J. Murray, and D. O. Huwe, Phys. Rev. Letters **10**, 179 (1963).
[11] L. Bertanza, V. Brisson, P. L. Connolly, E. L. Hart, I. S. Mittra, G. C. Moneti, R. R. Rau, N. P. Samios, I. O. Skillicorn, S. S. Yamamoto, M. Goldberg, J. Leitner, S. Lichtman, and J. Westgard, Phys. Rev. Letters **10**, 176 (1963).
[12] Detailed discussions of spark chamber construction and operation can be found in Rev. Sci. Instr. **30**, 482–531 (1961), and Nucl. Instr. Methods **20**, 143–219 (1963).

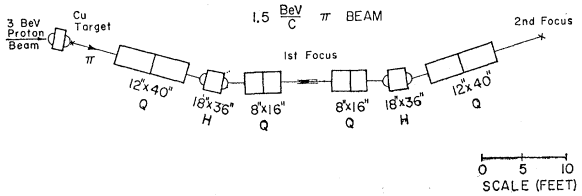

FIG. 1. 1.5-BeV/c π beam.

triggered the spark chambers when an interaction of the pion in the hydrogen target produced just neutral secondaries, one or more of which decayed in the main spark chamber.[13]

We wished to observe both decays

$$\Lambda \rightarrow p+\pi^-, \tag{2}$$

$$K_1^0 \rightarrow \pi^+ + \pi^-, \tag{3}$$

in the main spark chamber in order to completely investigate reaction (1). There was no attempt to look for gamma-ray conversions from the π^0. In fact, the chamber and counters were made with a minimum amount of material to decrease such gamma-ray conversions from π^0's produced by charge exchange. The coincidence counter (plastic scintillator) following the main spark chamber was large enough (12 in. diam) so that, for the case of $K^0\Lambda\pi^0$ production, the protons from the Λ decay had to traverse it. (In the case of $K^0\Lambda$ and $K^0\Sigma^0$ production, one or more of the decay products from (2) or (3) also had to go through the counter.) To look for triggering biases the counting efficiency across this last scintillator was tested using the pion beam and found to be greater than 98% over its entire area. The anticoincidence counter was found to be efficient enough; after adjusting the delay times of the counter pulses for satisfactory alignment (resolution time $\sim$5 nsec) the anticounter allowed a trigger only once every 40 000 pion traversals, and some of these were due to interactions in the target vessel or scintillator. We estimate that the actual anticoincidence failure rate was 1 in 10^5 π traversals.

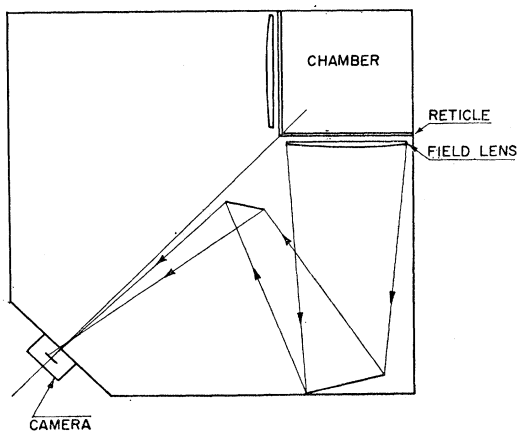

FIG. 2. Optical system. It is symmetrical about the diagonal. The spherical field lenses are machined out of Lucite.

[13] A similar triggering system was used by J. W. Cronin and O. E. Overseth in their Λ-decay parameter experiment. Phys. Rev. **129**, 1795 (1963).

Experimental Run

During the run, the time was split in the ratio 5/1 between hydrogen target full and empty. Triggers occurred at twice the rate with hydrogen as without. Longer background runs were not taken because it was felt our measurement accuracy would usually permit identification of an event origin as being inside or outside of the hydrogen, which turned out to be the case. With the target full, a picture was taken approximately once every three pulses. A total of 32 000 target-full pictures were obtained during the 9 day run; the corresponding number of scaler counts, measured only during the time a picture could have been taken, was 6.07×10^8.

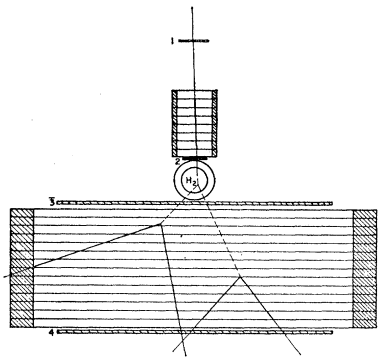

FIG. 3. Experimental arrangement. π^- incident from the top produces a Λ and K^0 which decay in the spark chamber. Counters 1, 2, and 4 are in coincidence and 3 is in anticoincidence to trigger the chambers on this type of event.

SCANNING AND MEASURING

Scanning

A photograph of one view of a double V event is shown in Fig. 4. The beam is incident from the top; the track of the incoming pion in the small spark chamber can be seen above the top reticle. The hydrogen target is just below between the two reticles, and the main spark chamber is approximately outlined by the lower rectangle of reticles. The large spark chamber had a gap efficiency of essentially 100% for pictures with four tracks, even for minimum ionizing particles in the presence of more heavily ionizing ones; the difference in ionization showed up in spark brightness.[14,15] For pictures with more than four tracks, the gap efficiency dropped below 100%, but double V's could be distinguished and measured even with a number of extra

[14] E. Engles, D. Roth, J. W. Cronin, and M. Pyka, IRE Trans. Nucl. Sci. NS-9, 256 (1962).

[15] C. T. Coffin, L. J. Curtis, D. I. Meyer, and K. M. Terwilliger, Nucl. Instr. Methods **20**, 156 (1963).

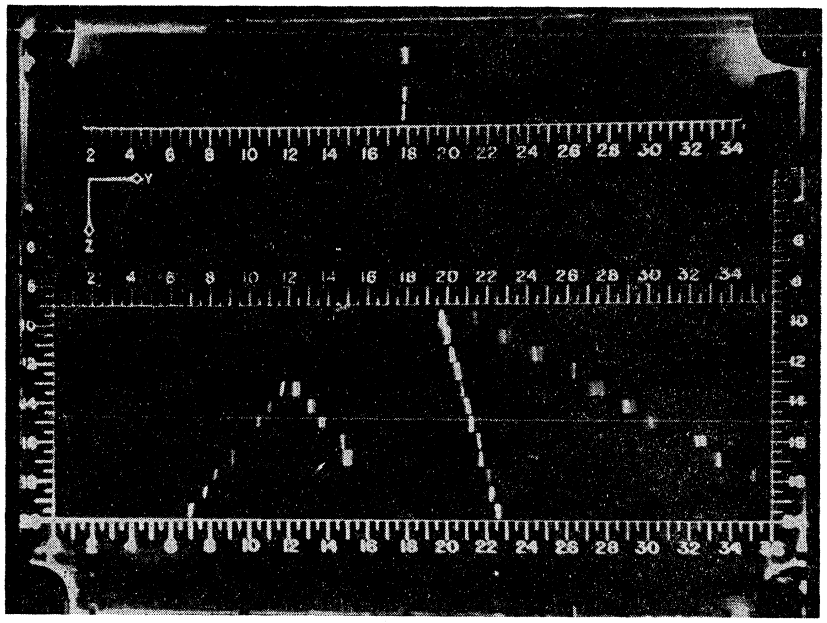

FIG. 4. Photograph of an event. The geometry is the same as in Fig. 3. The units of the reticle are cm.

tracks. When an event occurred it was alone in the photograph 60% of the time, and with 3 or more extra tracks only 4% of the time. Three percent of the events appearing to be double V's were unmeasurable, due to overlap or gap inefficiency.

All pictures were scanned twice. Comparison of the two scans indicated a single scan efficiency for double V's of around 98%.

Approximately 5% of the hydrogen pictures were double V events, 37% single V events, and the remainder were straight through tracks or charge exchanges; in the background run the number of double and single V's decreased to approximately 3% and 28%. These figures and the target full to empty triggering ratio (2/1) indicate that 3/5 of the V's from the hydrogen run were from the liquid hydrogen.

Measuring

Track identification and measuring were done at the same time as the scanning. Corresponding tracks were first identified in the two 90° views. This identification was usually obvious, through characteristically bright or dim tracks or occasionally missed gaps; it was rare that it was necessary to make use of the smaller angle stereo views. Measurement in most cases consisted in aligning a hairline with the sparks and manually recording coordinates from three intersections with the reticle system. For tracks going at small angles to the plates of the chamber, measurement accuracy of the azimuthal direction of the track was improved by recording the coordinates of corresponding sparks in the two views. All double V's that fired more than the two final gaps in the chamber were measured.

Each event was measured twice and the results were visually compared. A third measurement was made if the two measured track directions differed by more than $\frac{1}{2}°$ or 1°, depending on the angle of the track. After the comparison, the data from one of the measurements were punched on cards for analysis in an IBM-7090 computer.

DATA ANALYSIS

Spatial Reconstruction

Events were spatially reconstructed using the computer. There were three cross checks along the way to discover errors that had slipped by the two-measurement comparison and to find any "nonreal" events. A least-squares calculation checked the approximate collinearity of the three coordinate measurements on each view of a track while determining the best straight line through the measured points. Lines with a poor fit were remeasured until satisfactory. Then three-dimensional unit vectors for each track were computed from the slopes of the fit lines in the two views. The vertex of each V was overdetermined from the four lines in the two views, permitting a one constraint fit and a second check of measurement consistency. A third check was possible because the original event origin could be determined separately from each V by extending its plane back through the incoming pion line. After the two measurements of the origin were compared, a weighted average was found. The errors used in these last two consistency checks were computed by assigning an uncertainty to each line, the width depending somewhat on angle, but of order 1 mm. The measured χ^2 distributions were reasonable. Events which did not satisfy the above checks were re-examined and, if possibly real, were remeasured. If still not satisfactory

they were discarded; this, however, occurred rarely.

Fiducial volumes for acceptable events were established for the event origins and the V vertices. One of the constraints on the averaged event origin was that its position along the beam line could not be before or after the hydrogen target by more than its calculated error, which was usually around 3 mm. This constraint gave rise to a calculated loss of only 3% of true "inside target" events and permitted a good separation from background events occurring in the nearby Mylar windows and scintillation counters. The fiducial volume of the hydrogen target also required the π beam to be away from the lateral edges of the target and the edges of window in the stainless steel vacuum jacket. The decay fiducial volume was a cylinder, 10 cm long and 12 cm in radius, which required the V vertices to be more than $2\frac{1}{2}$ cm from the rear edge of the chamber, so that at least 3 gaps fired.

Initial Kinematic Analysis

The kinematic analysis was carried out in two steps, first a preliminary calculation to determine the nature of the event, then a best fit. From the experimental measurements, the directions of the incoming pion, the two neutral particles and their charged decay products are all known, along with the momentum of the incoming pion. If the identity of a neutral decaying to a V is assumed, its momentum is determined from the angles between it and its decay products. One neutral was assumed to be the K^0, the other the Λ. The reaction was analyzed as

$$\pi^-+p\rightarrow K^0+X^0, \tag{4}$$

the mass, momentum and direction of the X^0 being determined from the known 4-momenta of the other particles. The mass had to be consistent with a Λ^0, Σ^0, or $\Lambda^0+\pi^0$; in addition, the known direction and momentum of the Λ had to be consistent with its possible values from (4). Then the other neutral was chosen as the K^0 and the calculation repeated. The kinematics usually left no doubt as to the correct identification of the neutrals. The choice was confirmed and any ambiguities resolved with the use of the ionization information available in the track densities.

A plot of the measured mass distribution of the X^0 for the chosen assignment of the neutrals is shown in Fig. 5. A few grossly inconsistent events are not included. The background run indicates that about 15 of the Λ and Σ^0, and 15 of the $\Lambda\pi^0$ events are from outside the H_2 target. The Λ and Σ^0 peaks are clearly defined, with widths consistent with the estimated errors. The center of the Λ peak is 5 MeV below the accepted value of the Λ mass, 1115 MeV. This displacement was assumed due to error in our hot-wire measurement of the pion-beam momentum; a correction of this momentum from 1.500 BeV/c to 1.508 BeV/c, which moved the Λ peak to the accepted value, was made in all subsequent calculations.

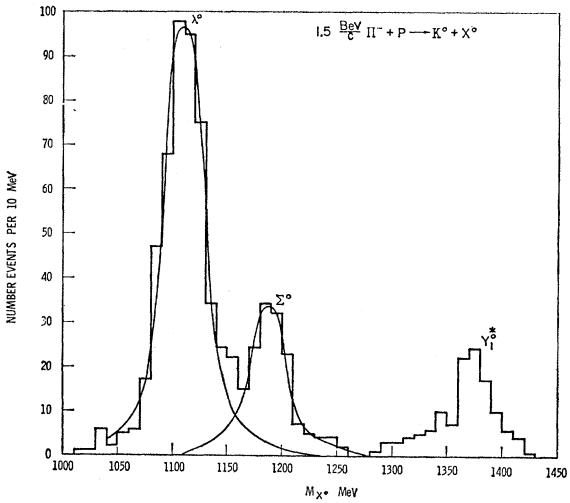

FIG. 5. Mass distribution of the X^0 in the reaction 1.5 BeV/c $\pi^-+p\rightarrow K^0+X^0$.

Events Best Fit as $K^0\Lambda\pi^0$

A best fit program,[16] with the hypothesis that the final state was $K^0\Lambda\pi^0$, was applied to all events with X^0 mass above 1250 MeV, the threshold. The event has one extra kinematic constraint. A nonkinematic constraint, that the event origins separately determined from the two decay V's be the same, made the program a two constraint fit. A quadratic twofold ambiguity in the Λ direction in the X^0 center of mass was resolved by fitting both ways, then choosing the one with minimum χ^2. The magnitudes of the originally assumed errors were adjusted slightly (downward 15%) to bring the χ^2 distributions from fitting the $K^0\Lambda$ and $K^0\Sigma^0$ events into agreement with theory; the $K^0\Lambda\pi^0$ events then also had the proper χ^2 distribution. The cutoff was taken at a χ^2 probability of 1%. Events outside this cutoff were remeasured. All acceptable events also had to be consistent with the ionization measurements.

127 events were finally classified as good, consistent with the $K^0\Lambda\pi^0$ hypothesis. Two events from the background run survived the fitting; with the factor of 5 difference in running time, this indicated that of order 10 of the 127 were from outside the hydrogen target.

Alternative Identifications

There are possible alternative identifications of some of the above events, even though they fit the $K^0\Lambda\pi^0$ hypothesis. Some could be $K^0\Sigma^0\pi^0$ or $K^0\Lambda\pi^0\pi^0$ if the mass of the X^0 is high enough; these alternatives can be distinguished using a χ^2 test only with a more precisely defined Λ momentum than our measurements gave. However, an estimate of the number of these alternative events can be made by examining the mass-squared

[16] Written by L. L. Yoder. Based on a general least-squares analysis by R. Böck, CERN 50–30, 1960 (unpublished).

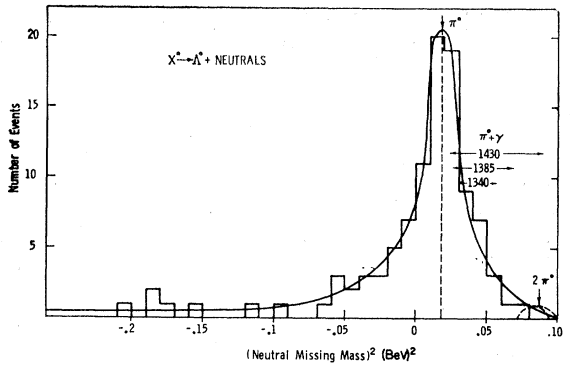

FIG. 6. Mass-squared spectrum of the missing neutrals in the reaction $X^0 \rightarrow \Lambda + \text{neutrals}$. The 4 momentum of the X^0 is obtained from the reaction $\pi^- + p \rightarrow K^0 X^0$. The neutral spectra for different possible X^0 decays are indicated. The solid curve is a π^0 resolution curve.

spectrum of the missing neutrals from the reaction

$$X^0 \rightarrow \Lambda + \text{neutrals}, \tag{5}$$

where the four-momenta of the X^0 and Λ are the original (nonbest-fit) values. The distributions expected when the neutrals are π^0, $\pi^0+\gamma$ (from $K^0\Sigma^0\pi^0$) or $\pi^0+\pi^0$ are indicated on Fig. 6, along with the measured distribution for all events with X^0 mass above the $\Sigma^0\pi^0$ threshold. The solid curve, a resolution curve, is the distribution expected for a π^0 and was obtained by perturbing the same set of events, best fit as $K^0\Lambda\pi^0$, with typical scanning errors. The measured distribution is consistent with being entirely events of the $K^0\Lambda\pi^0$ type, the admixture of the other reactions being approximately $0^{+7}\%$.

Error Calculations

In order to obtain estimates of errors in all the desired distributions, the fit events were perturbed by randomly generated scanning errors, then refit, with the same criteria used with the original data. Distributions of the fit-refit differences in quantities of interest were plotted, from which the expected errors in these quantities were found. With this data it was also possible to calculate the expected experimental distribution, smeared by errors, given an assumed theoretical distribution. This was done for a number of angular distributions; they were not markedly changed by the errors.

Bias Calculations

There were strong geometrical and triggering biases inherent in this experiment, but they were calculable and it was not necessary to resort to a Monte-Carlo procedure. The calculations determined (1) the probability that the K^0 and Λ would decay in the allowed fiducial volume, and (2) the probability that decaying in the allowed region, one of the decay products would not go back through the anticoincidence counter or into an unobservable region between the anticoincidence counter and the chamber. These calculations were made on an event by event basis. For the production distribution, however, the results were strongly dependent on statistical variations; a more realistic procedure which we used here was to calculate the probability of seeing a particular type of event, averaged over all quantities except the dependence desired. The average probability of seeing any event as a function of Y^* mass (for Y^* production center-of-mass angles $-1 \leq \cos\theta \leq 0.7$ and assuming an isotropic production angular distribution) is shown in Fig. 7(a), and as a function of Y^* center-of-mass production angle (for a Y^* mass of 1380 MeV) in Fig. 7(b).

Cross-Section Corrections

In order to obtain the $(Y_1^*)^0$ production cross section, it was necessary to make a number of corrections. The events observed in the selected $\Lambda\pi^0$ mass region 1340 to 1425 MeV (106) had to be adjusted for: (1) The probability of seeing the Λ and K^0, due to uncharged decay ($\frac{2}{3}$ for the Λ, $\frac{1}{3}$ for the K^0), (2) the probability of seeing an event due to geometric and triggering biases, given in Fig. 7(b), (3) out of target background, taken as 5%, (4) a 3% loss from events being unmeasurable, (5) a 1% scanning loss, and (6) 3% of the events lost because they occurred more than one standard deviation outside the target. The beam counts, 6.07×10^8, had to be corrected for: (1) A 3% pile up in the scalers, (2) muon contamination, assumed to be 5% from results from a similar beam setup,[17] and (3) 8% of the pions going through the counters but missing the fiducial volume of the H_2 target. The average target thickness seen by the beam, 2.5 cm, was found using the measured event origin distribution in the target.

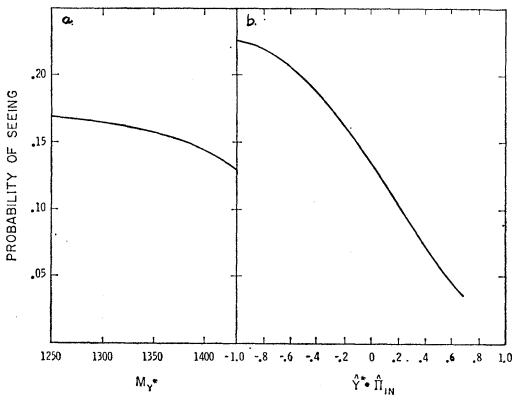

FIG. 7. Probability of seeing events due to geometric and triggering biases. (a) Probability as a function of the mass of the Y^*, averaged over center-of-mass production angles $-1 \leq \cos\theta \leq 0.7$. (b) Probability as a function of Y^* center-of-mass production angle. The mass of the Y^* here is 1380 MeV.

[17] R. Cool, O. Piccioni, and D. Clark, Phys. Rev. 103, 1082 (1956).

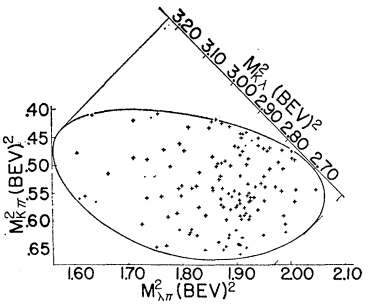

FIG. 8. Dalitz plot for 127 events best fit as $K^0\Lambda\pi^0$.

RESULTS AND DISCUSSION

The only final state appreciably produced in this experiment $1250 \leq M_{X^0} \leq 1436$, is $K^0\Lambda\pi^0$. There is no measurable amount of the $K^0\Sigma^0\pi^0$ state, indicating a relatively small production cross section for the 1405-MeV Y_0*.[18–20] [The $K^0\Sigma^0\pi^0$ state cannot be produced via $(Y_1^*)^0$ production and decay because of isotopic spin conservation.] The 1405-MeV Y_0* resonance is not evident in the X^0 mass spectrum either (Fig. 5).

Invariant Mass Distributions

All 127 "good" events best fit as reaction (1), are shown in a Dalitz plot in Fig. 8. The data are projected on to the three invariant mass axes in Fig. 9. The 1385-MeV Y_1* resonance clearly dominates the reaction. The data in the $\Lambda\pi^0$ mass distribution plot in Fig. 9(a) were fit using a maximum likelihood calculation to a resonance model of the form

$$dN/dM \sim A(M)P(M)[B+R(M)]. \qquad (6)$$

M is the $\Lambda\pi^0$ invariant mass; $R(M)=[(M-M_0)^2+(\Gamma^2/4)+\sigma^2]^{-1}$ representing the resonance spread by the experimental resolution, $\sigma=7.5$ MeV; B is a constant for the background; $P(M)$ is the probability of seeing an event of that $\Lambda\pi^0$ mass, M, assumed to be given in Fig. 7(a); $A(M)$ is three-body phase space. The parameters varied were M_0, Γ, and B. The fitted curve, the solid line in Fig. 9(a), has a χ^2 probability of 70%. The results are given in Table I. The dashed curves in Fig. 9(a), (b), and (c) are three-body phase space-times the probability of seeing the event. The resonance mass M_0 is quite consistent with the values from other experiments studying the charged Y_1*. The resonance width, Γ, appears significantly smaller than values obtained elsewhere, which are typically in the range of 50 MeV. However, a similarly narrow width was found by Berge *et al.*[2] in a low momentum (850 MeV/c) K^-p experiment. It is possible that our low result is partially due to a variation of the production-matrix element which is ignored in the Eq. (6) fit; for example, the production is consistent with being partly P wave (see below) and the centrifugal barrier could be cutting off the high side of the distribution faster than the assumed three-body phase space.

TABLE I. Parameters from maximum likelihood fit of a resonance model to the $\Lambda\pi^0$ mass spectrum.

M_0	1381±4 MeV
Γ	30±9 MeV
$B/R(M_0)$	$0.04_{-0.04}^{+0.05}$

106 of the 127 events are in the $\Lambda\pi^0$ mass region $1340 \leq M \leq 1425$ MeV and are assumed to be $(Y_1^*)^0$. The likelihood fit indicates that 8% of these are nonresonant background.

On the $K^0\Lambda$ and $K^0\pi^0$ invariant mass plots, Figs. 9(b) and 9(c), the solid curve is the $\Lambda\pi^0$ resonance distribution represented by Eq. (6) (and the solid curve of Fig. 9a) as reflected on the $K^0\Lambda$ and $K^0\pi^0$ mass axes. The general shapes of the two distributions are clearly in good agreement with the reflected resonance curve. However, there are apparently statistically significant (~3% probability) dips and rises around the positions of previously reported weak resonances,[21–23] 1650-MeV $K^0\Lambda$ and[7] 730-MeV $K^0\pi^0$, which might be the result of an interference between these weak resonances and the

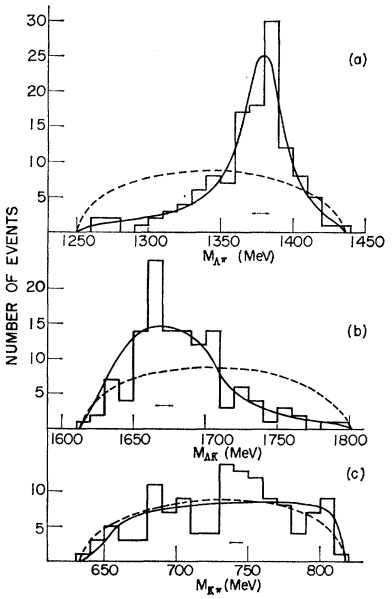

FIG. 9. Invariant mass spectra for events of Fig. 8. Dashed curves represent three-body phase space, solid curves the Y^* resonance model, all normalized to the total number of events.

[18] M. Alston, L. Alvarez, P. Eberhard, M. Good, W. Graziano, H. Ticho, and S. Wojcicki, Phys. Rev. Letters **6**, 698 (1961).
[19] P. Bastien, M. Ferro-Luzzi, and A. H. Rosenfeld, Phys. Rev. Letters, **6**, 702 (1961).
[20] M. Alston, L. Alvarez, M. Ferro-Luzzi, A. Rosenfeld, H. Ticho, and S. Wojcicki, *Proceedings of the International Conference on High-Energy Physics, CERN* (CERN, Geneva, 1962), p. 311.
[21] A. Baz, V. Vaks, and A. Larkin, Zh. Eksperim. i Teor. Fiz. **43**, 166 (1962) [translation: Soviet Phys.—JETP **16**, 118 (1963)].
[22] Ye. V. Kuznetsov, Ya. Shalomov, A. Grashin, and Ye. P. Kuznetsov, Phys. Letters **1**, 314 (1962).
[23] L. Bertanza, P. Connolly, B. Culwick, F. Eisler, T. Morris, R. Palmer, A. Prodell, and N. Samios, Phys. Rev. Letters **8**, 332 (1962).

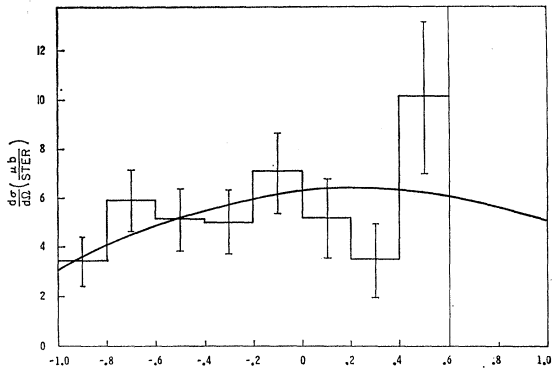

FIG. 10. Differential cross section for production of the $(Y_1^*)^0$. 106 events in the Y^* mass range $1340 \leq M \leq 1425$ MeV are used. The solid curve is a maximum likelihood S- and P-wave fit. Its equation is given in Table II.

strong Y_1^*. There is no indication of a significant tail from the 880 MeV K^*,[24] $\Gamma = 50$ MeV, in the $K^0\pi^0$ plot.

Production Cross Section of the $(Y_1^*)^0$

The center-of-mass differential cross section for production of the $(Y_1^*)^0$, $1340 \leq M \leq 1425$, is shown in Fig. 10. The histogram is the event distribution, corrected for the factors listed under data analysis. The cutoff is due to the very small probability of seeing K^0's produced backwards in the production center of mass; they go forward in the laboratory but usually decay before they reach the anticoincidence counter. The curve is a maximum likelihood fit, using just S and P waves since the center-of-mass momentum of the Y_1^* is only around 200 MeV/c. The fitted angular distribution is given in Table II, along with the total cross section (computed from the extended curve).

TABLE II. $(Y_1^*)^0$ production cross section.

$d\sigma/d\Omega$ μb/sr	$(6.3\pm0.9)[1+(0.15\pm0.27)\cos\theta-(0.35\pm0.38)\cos^2\theta]$
σ_{total} μb	(70 ± 11) μb

Spin of the Y_1^*

Recent experiments of Shafer, Murray, and Huwe,[10] and Bertanza *et al.*[11] have convincingly confirmed that the spin of the 1385 MeV Y_1^* is $\geq \frac{3}{2}$. Our angular distributions of the Λ in the Y_1^* center of mass are compatible with those results if we assume our Y_1^* production is not pure S wave. The Λ's are not significantly polarized so the polarization correlation method of analysis[10,25,26] is not available. The Λ distributions for all the Y_1^* events are shown in Fig. 11. The Λ directions were obtained in the usual way, by transforming from the laboratory to the production center of mass to the Y_1^* center of mass;[27] since the Y_1^* was produced near threshold, the last transformation was nonrelativistic. There is further evidence of a final state interaction in the large spike in Fig. 11(c), the left-right distribution. The events in the spike are mostly going up (positive $\hat{\Lambda}\cdot\hat{n}$) which is seen in the slight up-down asymmetry in Fig. 11(b). The spike includes many of the same events as the $K^0\pi^0$ peak. It is quite spread out in the front-back Adair distribution, Fig. 11(a), and is assumed to have a negligible effect there, as well as in the folded distribution of Fig. 11(b).

TABLE III. Maximum likelihood fits to folded Adair distributions for different production-angle regions. $z=\hat{\Lambda}\cdot\hat{\pi}$

Production angle range	Distribution
$1 \geq \lvert\cos\theta\rvert \geq 0.5$	$1+(1.1_{-0.7}^{+1.0})z^2$
$0.5 > \lvert\cos\theta\rvert \geq 0$	$1+(0.25_{-0.45}^{+0.60})z^2$
$1 \geq \lvert\cos\theta\rvert \geq 0$	$1+(0.60_{-0.45}^{+0.50})z^2$

Maximum likelihood fits to measured Adair distributions are given in Table III. Theoretical Adair distributions[28] for different spins, for S- and P-wave production,

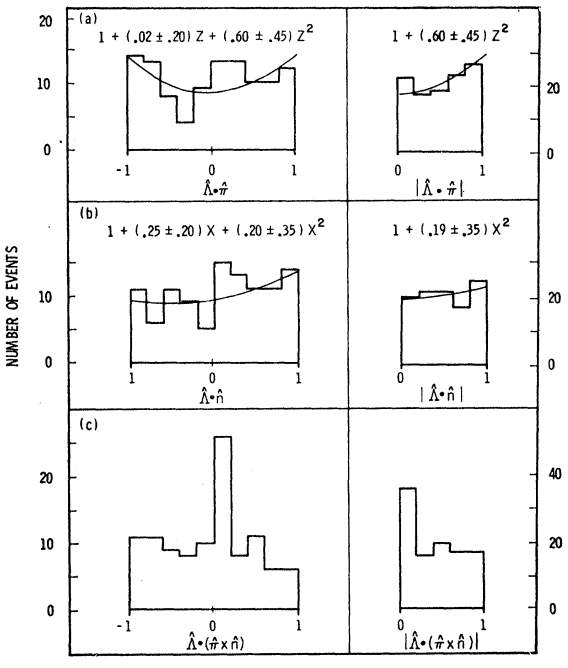

FIG. 11. Angular distributions of the Λ in the center-of-mass system of the Y_1^*. The solid curves are the maximum likelihood fits to the data. $\hat{n}=(\hat{\pi}\times\hat{Y})/|\hat{\pi}\times\hat{Y}|$, $z=\hat{\Lambda}\cdot\hat{\pi}$, $x=\hat{\Lambda}\cdot\hat{n}$.

[24] M. Alston, L. Alvarez, P. Eberhard, M. Good, W. Graziano, H. Ticho, and S. Wojcicki, Phys. Rev. Letters **6**, 300 (1961).
[25] R. Gatto, and H. P. Stapp, Phys. Rev. **121**, 1553 (1961).
[26] R. H. Capps, Phys. Rev. **122**, 929 (1961).
[27] H. P. Stapp, Phys. Rev. **103**, 425 (1956), and UCRL-8096, 1957 (unpublished).
[28] Some pertinent references in addition to 25 and 26 are: R. K. Adair, Phys. Rev. **100**, 1540 (1955); R. Spitzer and H. P. Stapp, Phys. Rev. **109**, 540 (1958); H. P. Stapp, UCRL-9526, 1960 (unpublished); M. Peshkin, Phys. Rev. **123**, 637 (1961); N. Byers and S. Fenster, Phys. Rev. Letters **11**, 52 (1963).

TABLE IV. Adair distributions for spins $\frac{1}{2}$, $\frac{3}{2}$, and $\frac{5}{2}$, for S and P wave production. $I(\theta)$ is the differential cross section for Y_1^* production. D is a P-wave coefficient. $|D|^2\sin^2\theta \leq I(\theta)$.

Spin	Distribution
$\frac{1}{2}$	1
$\frac{3}{2}$	$(1+3z^2)+\dfrac{2\|D\|^2\sin^2\theta}{I(\theta)}(1-3z^2)$
$\frac{5}{2}$	$(1-2z^2+5z^4)-\dfrac{\|D\|^2\sin^2\theta}{2I(\theta)}(1-18z^2+25z^4)$

are given in Table IV. The measured distributions are consistent with the theoretical for spin $\frac{3}{2}$ since P waves are not excluded in the production process. (For pure S wave, $D=0$, and our results would not be consistent with $\frac{3}{2}$.) For spins higher than $\frac{3}{2}$, the Adair distribution becomes more difficult to wash out with P-wave admixture; for $\frac{5}{2}$, it is quite asymmetric at any production angle, or averaged over any production-angle interval. We have examined the consistency of our data with spin $\frac{5}{2}$ by computing likelihood functions over the range of possible $\frac{5}{2}$ distributions. We find that, for the equatorial range $0.5>|\cos\theta|\geq 0$, the highest likelihood $\frac{5}{2}$ distribution has $\frac{1}{10}$ the probability of the $\frac{3}{2}$ distribution.

ACKNOWLEDGMENTS

We wish to thank Lavon Yoder for his assistance during the running and analysis of this experiment, including the writing of the computer best-fit program, and Michael Berggren and Dave Williams for their contributions in preparing and carrying out the run. We also wish to thank Dick Allen for his work on the error analysis program. We wish to express our gratitude to Lyle Smith, Bill Moore and the Cosmotron staff, who were very helpful throughout our stay at Brookhaven. Oreste Piccioni and his group, with whom we alternated in their beam, were extremely cooperative. The hydrogen target was kindly loaned to us by Sid Warshaw and Al Wattenberg.

PHYSICAL REVIEW VOLUME 132, NUMBER 4 15 NOVEMBER 1963

ΛK^0 and $\Sigma^0 K^0$ Production in 1.5-BeV/c $\pi^- p$ Interactions*

L. L. YODER, C. T. COFFIN, D. I. MEYER, AND K. M. TERWILLIGER
The University of Michigan, Ann Arbor, Michigan
(Received 15 July 1963)

476 ΛK^0 and 134 $\Sigma^0 K^0$ events have been investigated in the experiment 1.508 BeV/c $\pi^- p \to \Lambda K^0$ and $\Sigma^0 K^0$. The Λ is produced mostly backward in the center of mass and has an average polarization (-0.76 ± 0.14). The production and polarization angular distributions are well fit with *spd* waves. The total ΛK^0 production cross section is $(214+23)$ μb. The Σ^0 production angular distribution has a small backward peak and an indication of a forward rise; it is consistent with either *sp* or *spd* waves. The statistics are too poor to measure the Σ^0 polarization.

INTRODUCTION

THERE has been a considerable amount of data collected on the associated production reaction[1-9]

$$\pi^- + p \to K^0 + \Lambda. \qquad (1)$$

Most of it has been obtained with pion momenta <1250 MeV/c. The published data on the reaction

$$\pi^- + p \to K^0 + \Sigma^0 \qquad (2)$$
$$\Sigma^0 \to \Lambda + \gamma$$

* Supported by the U. S. Atomic Energy Commission.

[1] F. Crawford, M. Cresti, M. Good, M. Stevenson, H. Ticho, G. Kalbfleisch, and R. Douglass, in *Proceedings of the Ninth International Conference on High-Energy Physics at Kiev, 1959* (Academy of Science, USSR, Moscow, 1960), p. 444.

[2] J. A. Anderson, F. S. Crawford, B. B. Crawford, R. L. Goldon, L. J. Lloyd, G. W. Meisner, and R. L. Price, in *Proceedings of the 1962 Annual International Conference on High-Energy Physics at CERN* (CERN, Geneva, 1962), p. 270.

[3] L. Bertanza, P. L. Connolly, B. B. Culwick, F. R. Eisler, T. Morris, R. Palmer, A. Prodell, and N. P. Samios, Phys. Rev. Letters **8**, 332 (1962).

[4] F. Eisler, R. Plano, A. Prodell, N. Samios, M. Schwartz, J. Steinberger, P. Bassi, V. Borelli, G. Puppi, H. Tanaka, P. Waloschek, V. Zobali, M. Conversi, P. Franzini, I. Mannelli, R. Santangelo, and V. Silvestrini, Nuovo Cimento **10**, 468 (1958).

[5] J. L. Brown, D. A. Glaser, and M. L. Perl, Phys. Rev. **108**, 1036 (1957).

[6] Collaboration: Saclay, Orsay, Bari, and Bologne, in *Proceedings of the Aix-en-Provence International Conference on Elementary Particles* (Centre d'Etudes Nucleaires de Saclay, Seine et Oise, 1961), Vol. 1, p. 375.

[7] R. K. Adair and L. B. Leipuner, Phys. Rev. **109**, 1358 (1958).

[8] M. I. Soloviev, in *Proceedings of the 1960 International Conference on High-Energy Physics at Rochester* (Interscience Publishers, Inc., New York, 1960), p. 388.

[9] J. Bartke, R. Bock, R. Budde, W. A. Cooper, H. Filthuth, Y. Goldschmidt-Clermont, F. Grard, G. R. MacLeod, A. Minguzzi-Ranzi, L. Montanet, W. G. Moorhead, D. R. O. Morrison, C. Pezrou, B. W. Powell, J. Trembly, D. Wishott, I. Bertanza, C. Franzinetti, I. Mannelli, V. Silvestrini, G. Brautti, M. Ceschia, and L. Chersovani, in *Proceedings of the 1960 International Conference on High-Energy Physics at Rochester* (Interscience Publishers, Inc., New York, 1960), p. 402.

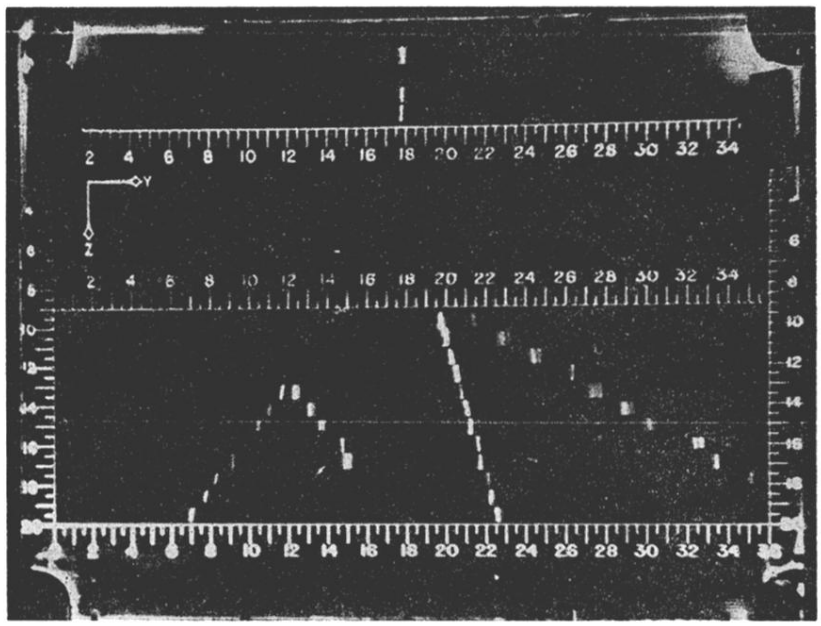

FIG. 4. Photograph of an event. The geometry is the same as in Fig. 3. The units of the reticle are cm.